Experimental Assessment of the Viability of Sugarcane Bagasse Fiber Usage as Sound Absorbing Component of Standard Concrete for Environmental Noise Mitigation

Babashola D ODUGBOSE, Herni HALIM*, Izwan JOHARI, Wan Mohd Amri Wan MAMAT ALI

Abstract—**This study aims to evaluate the impact of incorporating sugarcane bagasse fiber (SBF) in concrete on the resulting natural fiber composite concrete's sound absorption performance and mechanical properties. The sugarcane bagasse fiber concrete (SBF-C) was fabricate using varying SBF content (0%-5%) as a substitute for fine aggregates by volume content. Plain concrete (PC) and produced SBF-C were evaluated to examine workability, mechanical properties, sound absorption coefficients, and durability properties. The addition of SBF significantly enhanced the sound absorption performance of concrete. The sound absorption coefficient (SAC) increased with percentage increments of 28%, 55%, 58%, 65%, and 74% as the fiber content increased, compared to plain concrete. SBF incorporation reduced workability and increase compressive strength at 1-2% fiber content followed by reduction of strength at higher fiber content, caused a slight increase in flexural and splitting tensile strength at low fiber content, and increased porosity and water absorption as fiber content increased. Due to SBF incorporation, the rise in SAC of the concrete makes the composite concrete usable as a noise barrier for noise pollution mitigation.**

***Index Terms*— Concrete's compressive strength, Environmental noise pollution, Sugarcane bagasse fiber-concrete (SBF-C), Sound absorption coefficient (SAC)**

I. INTRODUCTION

The primary environmental challenges in the world are sound pollution, water pollution, air pollution, and solid waste pollution [1]. The phenomenon known as environmental noise, also called sound or noise pollution, has recently received increased recognition due to the migration of people from rural to urban regions, resulting in rapid urbanization worldwide [2]. This migration is linked to transitioning into an economy centered around manufacturing, technology, and services. The swift urbanization and proliferation of many city amenities have amplified noise levels [3]. The significant rise in noise levels is linked to road, train, and aviation activity. Road traffic is the primary noise source, surpassing the total noise levels from rail and airplane sources [4]. Indeed, in metropolitan settings, automobile traffic is estimated to contribute approximately 80% of total noise pollution [5]. Hence, reducing the noise levels caused by road traffic while designing urban areas is crucial. Excessive noise can have detrimental effects on human health. Recent measures have been implemented to regulate noise and vibrations [6]. Ensuring acoustic comfort is a crucial aspect of urban comfort and an essential task in civil engineering and urban planning. Hence, the reduction of ambient noise holds great significance in contemporary society, not only due to its substantial health risks but also because of its increasingly crucial impact on the overall level and quality of life [7]. The change in perception is primarily attributed to recent studies demonstrating the detrimental effect of environmental noise exposure on various health aspects. According to various research outputs [8]–[18], the adverse effects include cardiovascular diseases, sleep disturbances, cognitive impairment in children, psychological disorders, auditory system impairment, obesity, noise-induced hearing loss, hypertension, and more.

Research is being conducted using a circular economy to produce non-synthetic noise barriers. This approach involves promoting the development of new technologies and updating traditional manufacturing processes to address the health issues caused by excessive exposure to environmental noise. This economy relies on the utilization of waste materials in novel manufacturing chains or processes, as well as the development of new materials. The objective is to decrease expenses associated with trash disposal and minimize the environmental impact by limiting the excessive utilization of natural resources, which may include non-renewable sources [19]. Hence, it is crucial for sustainable development to utilize materials that are readily biodegradable, locally available, and ecologically beneficial. This category includes fibrous materials, such as fibers derived from biological sources, and any further processing done with minimal or dangerous effects [20]-[21].

Manuscript received May 23, 2024; revised November 12, 2024.

This work was supported by Universiti Sains Malaysia (USM) through the Research University Individual-RUI Grant (1001/PAWAM/8014161).

B.D, Odugbose is a PhD candidate at the School of Civil Engineering, Kampus Kejuruteraan, Universiti Sains Malaysia, 14300, Nibong Tebal, Pulau Pinang, Malaysia. (e-mail: odugbose.babashola@student.usm.my; odugbosebabashola@yahoo.com)

H. Halim is a Senior lecturer in the School of Civil Engineering, Kampus Kejuruteraan, Universiti Sains Malaysia, 14300, Nibong Tebal, Pulau Pinang, Malaysia. (Corresponding author phone: +6-04-5996247; email: ceherni@usm.my, HerniHalim@yahoo.com).

I. Johari is a Senior Lecturer in the School of Civil Engineering, Kampus Kejuruteraan, Universiti Sains Malaysia, 14300, Nibong Tebal, Pulau Pinang, Malaysia. (e-mail: ceizwan@usm.my).

Wan Mohd Amri Wan Mamat Ali is a Researcher Officer in the Vibration Laboratory, School of Mechanical Engineering, Engineering Campus, Universiti Sains Malaysia, 14300, Nibong Tebal, Pulau Pinang, Malaysia. (e-mail: amri@usm.my)

Concrete, the primary construction material of our era, has been overlooked in uses as a substitute for synthetic noise barriers, which can easily be used for sound absorption in building facades, interior partitions, and urban planning, such as the construction of soundproof fences along high-speed roads [22]-[23]. The sound absorption coefficient quantifies concrete's capacity to hinder sound propagation. A more significant absorption coefficient signifies that the concrete is efficient in sound isolation. Rodrigues et al. [24] reported that the sound absorption coefficient of concrete ranges from 0.05 to 0.10. While mineral wool, glass wool, polyester, polyurethane, and other synthetic materials effectively absorb sound in sound absorbers, their usage in concrete formulation for improvement is limited due to health risks, expensive manufacturing, and negative environmental impacts [25]. The replacement of these materials is centered around using environmentally friendly products that are plentiful, biodegradable, and possess mechanical and acoustic benefits. Additionally, it serves as an effort to implement new building standards to enhance sustainability and develop environmentally friendly construction materials [26]-[27].

The rising popularity of natural fibers can be attributed to the higher cost of industrialized fibers and the imperative to mitigate the detrimental environmental impact of the construction sector [28]. Sugarcane bagasse fibers (SBF) have recyclable, renewable, and eco-friendly properties, making them a viable and sustainable natural resource for utilization in the building industry, similar to other natural fibers. Specifically, "natural fiber" refers to plant-derived materials such as seed, bast, leaf, fruit, stalk, grass/reed, and wood. These materials have been identified as potential sources for producing new sound absorbers [29]. A study by Wang et al. [30] found that the use of a composite consisting of wheat straw, rice husk, and sawdust in a metakaolin-geopolymer-based insulation material had an improved sound absorption coefficient of 0.71 at a frequency of 1028 Hz. Chen et al. [31] found that when 2-4 mm miscanthus fibers are added to miscanthus lightweight concrete, the acoustic absorption improves. As the content of miscanthus fibers increases, the sound absorption coefficient also increases significantly, reaching values between 0.28 and 0.63.

In a separate investigation by Chen et al. [32], incorporating miscanthus fiber into ultra-lightweight concrete led to a significant acoustic absorption coefficient of 0.9 at low frequencies, indicating that the concrete is suitable for acoustic absorption. Still, its use is limited to non-structural applications in civil engineering. According to the study by Pachla et al. [33], adding rice husk and rice straw to a cellular concrete composite improved its ability to absorb sound. The composite exhibited the highest absorption coefficients at low frequencies ranging from 50 to 1250 Hz, with sound absorption coefficients ranging from 0.20 to 0.45 for different fiber compositions. In comparison, plain concrete had absorption coefficients ranging from 0.05 to 0.09. Oancea et al. [34] demonstrated that incorporating corn cob and sunflower fiber in concrete enhances its sound absorption coefficient to 0.20 – 0.24, compared to plain concrete, which typically has a coefficient of 0.10 – 0.16. This improvement, although minor, is optimistic.

The research findings indicate that incorporating natural fiber into concrete positively impacts sound absorption. However, further investigations are being conducted to explore materials that offer superior acoustic performance and are structurally suitable for construction projects. To this end, the authors acknowledge the gap in the literature as no scientific literature reports of research investigating the acoustic qualities of concrete containing sugarcane bagasse fiber (SBF) exist. This work seeks to analyze the utilization of SBF as a sound-absorbing material in concrete composites and explore the sound absorption coefficient of these composites.

II. MATERIALS AND METHODOLOGY

A. Materials

The materials used to modify standard concrete into sound, absorbable, sustainable concrete include ordinary Portland cement, coarse aggregate (gravel, maximum size of 20 mm), fine aggregate (river sand), water, and sugarcane bagasse. Sugarcane bagasse fiber was used primarily to partially replace fine aggregate in the concrete constituents' material composition. Fig 1, illustrates the sugarcane bagasse sourcing and the microstructural image of SBF using scanning electron microscopy (SEM).

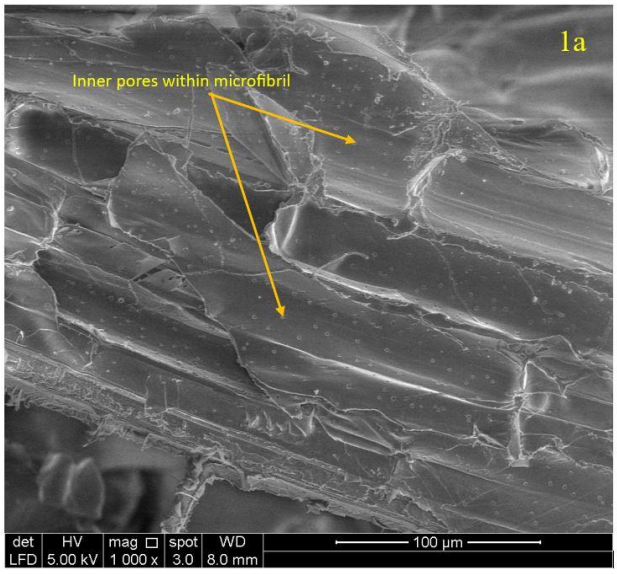

Fig 1. Sugarcane Bagasse: (a) Scanning micrograph of sugarcane bagasse (b)Wet sugarcane bagasse collection

B(i). Methodology

The concrete mixes were formulated following the standards outlined in ACI 318 [35], with which a design mix ratio of 1: 1.62: 2.33: 0.45, representing ratios of cement, fine aggregate, coarse aggregate, and water, respectively, was obtained. The fiber sourced underwent a drying process in the oven for 72 hours to remove excess moisture, followed by size reduction using a crusher. The ground fiber was further sieved to get a size that could fit through a sieve with a diameter of 1.19 mm, resulting in a fiber size range of 0 - 1.18 mm.

The decision was made to utilize the diameter sieve passage size instead of the fiber length since the fiber had undergone a torsional size reduction within the oil extruder machine. This reduction had a noticeable impact on the fiber length, leading to inconsistent output in terms of fiber length. The selected fiber size falls within the allowed range of sizes for fine aggregate. The fiber was incorporated into the mixture by partial replacement of the fine aggregate content at different loadings, specifically 1%, 2%, 3%, 4%, and 5%, replacing fine aggregate by volume content, respectively. This technique of partial replacement was motivated by prior studies undertaken by Karolina et al. [36].

B(ii). Concrete Specimens Production

The ratios for the components of the concrete mixture for a volume of 1 cubic meter ($1m^3$) are specified in Table I. Adhering to the constituent mix proportion as expressed in Table 1, respective components were weighed. Cement and fine aggregate were mixed in dry state inside a concrete mixer for 1 minutes. Thereafter, sugarcane bagasse fibre was added into the mixture and further mixed for additional 1 minutes. Subsequently, coarse particles added, and water was incrementally added with a continuous mixture for additional 2-3mins until a completely mixed wet-composite concrete was obtained. Prior to molding, the slump test was conducted in accordance with ASTM C143/C143M [37] standard to ascertain the workability of the fresh composite concrete

The wet specimen was cast in prepared oil-smeared moulds in three layers, with each layer undergoing mechanical agitation using an electrically powered vibration table to facilitate compaction; carried out for the different molds for each specific test in accordance with standards. After 48-hour, the specimens were removed from the moulds and place in water tank for water-based curing which were then left in the tank till minutes prior to testing at the different testing ages.

Table I: Composition of Concrete Mix (kg/m^3) at w/c (0.45) For SBF-C

Sample	Cement	River Sand	Coarse Aggregate	Weight (%)	Fiber Weight	Water
OPC0	440.5	714	1024		0	196
SBF-C1	440.5	706.9	1024	1	1.964	196
SBF-C2	440.5	699.7	1024	2	3.928	196
SBF-C3	440.5	692.6	1024	3	5.893	196
SBF-C4	440.5	685.4	1024	4	7.863	196
SBF-C5	440.5	678.3	1024	5	9.821	196

C. Testing

C(i). Mechanical, Physical and Durability Properties

The density and water absorption of plain concrete and SBF-C were determined per ASTM C642-21[38]. Compressive strength testing was performed according to the BS EN 12390-3 [39] standard at 7, 14, and 28 days. Flexural strength and splitting tensile strength tests were conducted following ASTM C 78-02 [40] and ASTM C 496/C 496M – 04 [41], respectively, at a concrete cured age of 28 days. RCPT were conducted in accordance with ASTM C1202 [42] with cured concrete of ages 28 and 56 days respectively

C(ii). Sound Absorption Coefficients of SBF-C

The produced sugarcane bagasse fiber concrete's sound absorption coefficient (SAC) was evaluated using the standing wave method with an impedance tube, following ASTM E 1050 [43] standards. Other researchers previously employed this method in their acoustic studies [44-45] of cementitious composite materials. The sound absorption coefficient (SAC) of ordinary Portland cement (OPC) concrete and SBF-C-(1%-5%) was measured using the Spectronics ACUPRO Impedance Tube, part number F-SPEMCIUS-G, which has an inner diameter of 34.8 mm. The measurements were conducted using the Siemens LMS 8-Channel Test Lab System SCADAS hardware with DAC output. The test covered a frequency range of 50 Hz to 5600 Hz and was performed after the samples had cured for 28 days. The test specimens have the exact dimensions as the inner diameter of the tube. Before the test, the microphones were calibrated using the GRAS Sound & Vibration Class 1 Sound Calibrator, specifically the GRAS 42AG model with serial number 279131. The calibrator was set to produce a sound frequency of 1000 Hz with an accuracy of ± 0.1 Hz and a sound level of 94.0 dB with an accuracy of ± 0.1 dB. This calibration was done to ensure precise measurement of sound pressure within the tube.

Each percentage replacement of fine aggregate was tested using three specimens, and the measurement was done three times to guarantee repeatability and reproducibility. For every measurement, the sample was taken out and then put back into the sample holder, and it was determined that the variability was insignificant for all samples. Fig 2, illustrates the pictorial view of the laboratory impedance tube configuration for the acoustic performance determination.

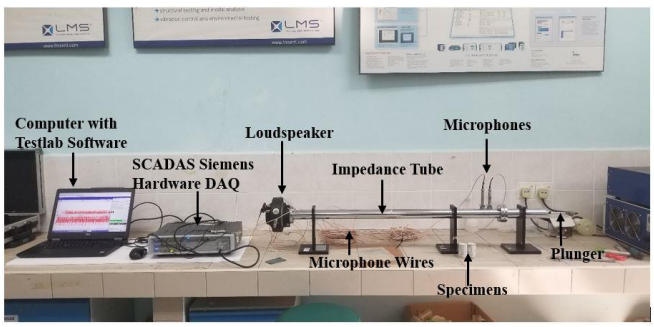

Fig 2. Siemens LMS SCADAS Impedance Tube Setup in Laboratory.

The sound absorption average (SAA) is a single value representing the sound absorption coefficient and can be obtained by calculating the average of twelve 1/3th octave

band frequencies, primarily within the 200 - 2500 Hz range. The derivation of SAA can be achieved by referring to (1), previously utilized by Samaei et al. [46] in a separate study. An alternative method for quantifying SBF-concrete's overall sound absorption properties is to use the noise reduction coefficient (NRC) value, which serves as the basis of comparison in sound-absorbable materials and is derived using the expression in (2). This approach has been previously used by Nastac et al. [47] and Raj et al. [48].

$$SAA = \frac{\sum \alpha \, at \, \frac{1}{3th} \, octave \, band \, center \, frequencies}{n} \quad (1)$$

Where,

SAA = Sound Absorption Average
α = Sound Absorption Coefficient
n = numbers of selected octave band

$$NRC = \frac{(\alpha_{250}+\alpha_{500}+\alpha_{1000}+\alpha_{2000})}{4} \quad (2)$$

Where,
NRC = Noise Reduction Coefficient
α_{250}, α_{500}, α_{1000} and α_{2000} = sound absorption coefficient at frequencies of 250 Hz, 500 Hz, 1000 Hz, and 2000 Hz.

C(iii). Porosity of Acoustic Properties Specimens

The porosity is determined according to the parameters provided in ASTM C830-00 [49]. This procedure detects empty spaces within the specimens that may enhance their ability to absorb sound. A material's acoustic absorption capabilities depend on open voids within it, making the porosity a reliable measure for evaluating its performance [50]. Thus, the specimen employed to determine the sound absorption coefficient was also used to conduct the porosity test.

C(iv). Morphological Properties and Elemental Analysis

The morphological properties of concrete entails the critical study of the concrete microstructure, understanding the interconnectivity and bonding of the different constituents utilizing both scanning electron microscopy SEM and energy dispersive x-ray spectroscopy (EDX). An acoustic specimen measuring 1 cm x 1 cm was analyzed using a scanning electron microscope (SEM) to investigate the impact of fibers on the microstructure of SBF-concrete and to identify any potential formation of pores in the composite concrete. The specimen was attached to a holder using adhesive carbon tape. The analysis was conducted utilizing an FEI QUANTA FEG 650 scanning electron microscope machine with serial number D9817, operated at 5 kilovolts (kV) at 1000 magnifications to obtain the micrograph image. EDX offers elemental analysis with a high level of precision, even in areas as small as a few nanometers. EDX enables the identification of the elemental composition of specific locations or the spatial distribution of elements by utilising the scanning function of the electron microscope [51]. This analysis was conducted o same specimens used for SEM concurrently.

C(v). Thermogravimetric Analysis

Thermal analysis (TA) as a group of techniques that monitor changes of physical or chemical properties of a sample with time as it undergoes a temperature program. Thermogravimetric analyzers (TGA) monitor and record sample mass, time, and temperature. The Thermogravimetric analysis (TGA) test of the specimens was conducted using Shimadzu DTG-60/60H machine to assess hydration characteristics of concretes fabricated and effect of the partial replacement of the fine aggregate content on the hydration process by studying changes in hardened concrete comparable to procedure by Kaddah et al. [52]. Samples were prepared by crushing prepared specimens in jaw crusher and then sieving the crushed specimen to obtain powder (passing 75µm sieve) size. Test samples weighing approximately 20 mg were inserted in a platinum pan specimen holder, and the apparatus is operated by heating at 10°C/minutes up to 1000°C

III. RESULTS AND DISCUSSIONS

A. Concrete Physical Properties

Ai. Slump

The slump of sugarcane bagasse fiber concrete (SBF-C) specimens and that of regular standard concrete (OPC) specimens were evaluated following ASTM C143. Fig 3, shows the slump of the specimens and the slump range. The incorporation of sugarcane bagasse fiber in standard concrete reduced the slump. The highest and the lowest slumps were obtained in plain concrete (245.8 mm) and SBF-C-5% (133 mm) specimens. The effect of SBF on the workability of concrete using the slump test shows a reduction trend in the slump values obtained for the fresh concretes as the loading of fiber increases.

A reduction percentage in slump amount to 3.4%, 13%, 23%, 34%, and 46%, representing fiber loads of 1, 2, 3, 4, and 5%, respectively, ensued in reinforced concrete compared to control. The results indicated that sugarcane bagasse fiber negatively affects the rheological properties of fresh standard concrete when incorporated into it and, ultimately, reduces workability. The reduction in workability of sugarcane bagasse fiber-reinforced concrete attained in this study is akin to reduction in the slump value of coconut fiber-reinforced concrete, as reported by Ali et al. [53], with a 27-82% reduction compared to plain concrete. SBFs absorb large amounts of water due to the high specific surface area and hydrophilic nature of the fiber, reducing the water needed to improve the mixture flow.

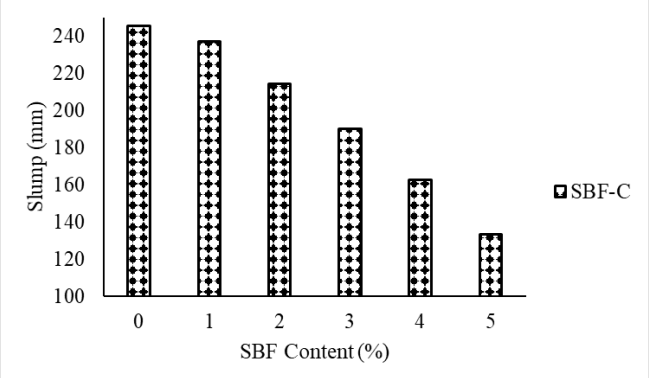

Fig 3. Fresh SBF-C Workability (Slump) Test

***Aii.* Density**

Fig 4, illustrates the impact of incorporating sugarcane bagasse fiber as a partial replacement for sand, replacing the equivalent percentage substitution by volume content of replaced fine aggregate on the densities of the resulting composite concrete. After 28 days of curing, the test results indicate a consistent reduction in the concrete density as the amount of fiber increases. The density values of SBF-C were measured at 2335.87 kg/m3, 2303.8 kg/m3, 2301.5 kg/m3, 2247.7 kg/m3, and 2249.9 kg/m3. These values represent a percentage reduction compared to the density of the control specimen (2346 kg/m3) at 0.43%, 1.81%, 1.90%, 4.20%, and 4.11%, corresponding to fiber-sand replacements of 1%, 2%, 3%, 4%, and 5%, respectively. This decrease in density can be attributed to the lower density of the fibers compared to that of river sand. The reduction in density seen in this study is similar to those reported by Ahmed [54] and Subedi et al. [55], in which partial replacement of sand in the concrete with natural fiber decreased density. The findings of this study indicate that a decrease in the density of concrete can lead to a reduction in its structural strength, durability, and ability to withstand environmental influences.

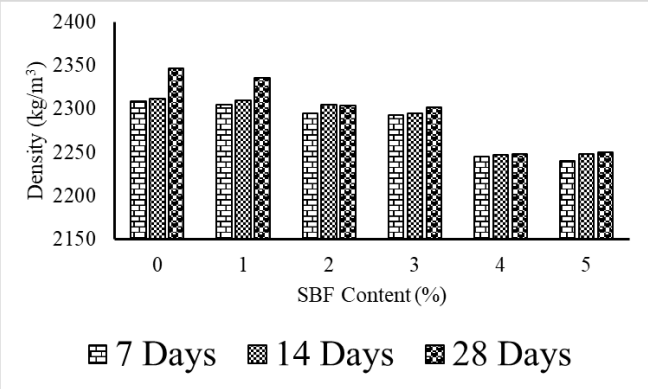

Fig 4. Density of SBF-C

Aiii. Rapid Chloride Penetration Test

The durability of concrete can be affected by the actions of chloride penetration in and within the concrete and the resistance of this penetration can be studied using the rapid chloride permeability test (RCPT). Fig 5, illustrates the resistance capabilities of produced SBF-C on the penetration of chloride ion expressed in charge passed (coulomb) at 28 and 56 days cured specimens.

At 28 days, cured SBF-C shows an initial reduction of chloride penetrability from the plain concrete compared to 1% sugarcane bagasse fiber concrete penetrability. Subsequently the chloride penetrability restriction is less evident by the increase in the charge passed as the fiber content increases. The RCPT value range of 5125 coulombs to 5900 coulombs at the various fiber loading rate was attained compared to plain concrete with RCPT value of 5614 coulombs. A percentage difference range of -8.72%, -4.09%, -0.23%, +3.04% and +5.09% representing concrete fabricated with fiber contents 1, 2, 3, 4, and 5% respectively compared to plain concrete chloride penetrability potential.

56 days cured specimens takes the same graph trend of that obtained at 28 days with an initial reduction in the total charge passed at 1% fiber content compared to plain concrete, after which a steady rise in chloride ion penetrability ensued as the fiber content increase. In comparison to the charge passed of plain concrete, a percentage variation of -13.21%, -12.08%, -10.58%, -8.31% and +11.14%, respectively representing fiber contents 1, 2, 3, 4, and 5% is obtained. The result of this study shows that SBF-C possess little resistance to chloride ion penetrability as all the charge passed are classified as moderate to high penetrability in accordance with standard.

The result contradicts that reported by other researcher Mohamed & Hawat, [56] which reported an increase in resistance to chloride passage on concrete produced with 40% fly ash content with 1% – 2% blast fiber addition loading. Likewise with the report of result from study conducted by Priya & Sudalaimani [57] which reported an increase in chloride ion resistance due to densification of the specimen after incorporation of fiber. However, comparing 28 days to 56 days cured specimens shows a reduction in the chloride charge passed as the curing days increased which is a significant improvement in the resistance of penetrability of chloride ion, corroborating Zeyad et al. [58] which stated that increase in the age of curing leads to better resistance of chloride ion permeability in older cured concretes. The variation in these two values corroborate the effect of age of concrete on the penetrability of chloride ion.

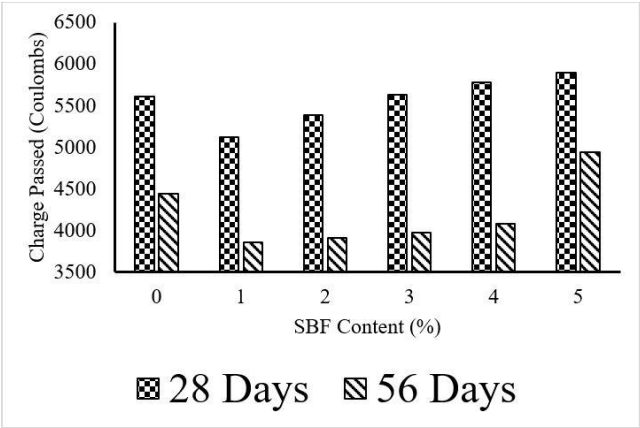

Fig 5: Rapid chloride penetration test (RCPT)

B. Mechanical Properties

Bi. Compressive Strength (CS)

The mean compressive strength value of three specimens each for the different fiber loading of sugarcane bagasse fiber concrete specimens and that of the control specimens at 7, 14, and 28 days are presented in Fig 6. A variation in the effect of sugarcane bagasse fiber on compressive strength was observed at different cured ages of concrete, but a general reduction in compressive strength ensued at high fiber contents. The compressive strength of specimens of sugarcane bagasse fiber concrete at 7-days containing 1, 2, 3, 4, and 5% fiber increased by 0.33% at 1% fiber content, then subsequent increases in fiber content led to reductions by 52.77, 90.04, 94.18 and 93.00% at fiber loading of 2, 3, 4, and 5% respectively. The use of 1, 2, 3, 4, and 5% fiber content in regular standard concrete at 14 days of age exhibited the same pattern as that of 7 days in which a fiber load of 1% led to an increase in compressive strength at 3.85% compared to the control value. Further increases in fiber contents at 2, 3, 4, and 5% reduced compressive strength by 45.36, 88.55, 94.69 and 94.10%, respectively. At 28 days of cured concrete, the fiber addition at 1% and 2% loading resulted in the slight increase in the compressive

strength with percentages increment of 3.28% and 0.66% respectively while fiber loading 3, 4 and 5% exerts a reduction in the compressive strength to the tune of 58.73, 91.54 and 92.95% respectively.

The presence of sugarcane bagasse fiber in standard concrete exerts a positive influence at an optimum loading 1-2%, further increase in the fiber load reduces the bonding of the aggregates in the matrix and results in lower force transmission. The use of sugarcane bagasse fiber has a significant effect on compressive strength, exerting a reduction due to a reduction in the transition zone's strength and the aggregate's inability to adhere to the fiber and other constituents due to the fiber's absorption of free water within the microstructure of the concrete thereby reducing hydration process and entrapment of air leading to a reduction in strengths. The effect on compressive strength, as expressed in this study at high fiber loading, corroborates the study conducted on oil palm mesocarp fiber concrete conducted by Odugbose et al. [59] in which compressive strength reduces in the range of 10-36.98% as the fiber inclusion increases. In the work of Shon et al. [60], a 26.2-56.8% reduction in compressive strength ensued as common reed fiber content increased in the common reed fiber reinforced concrete. Mixing sugarcane bagasse fiber in concrete and its incremental content volume leads to the observed defects in the concrete strength. Also, increased fiber content in the mixture causes the balling phenomenon and improper distribution of fibers in concrete. In addition to reducing the workability of concrete, this action creates porosity (resulting from improper compaction) in concrete.

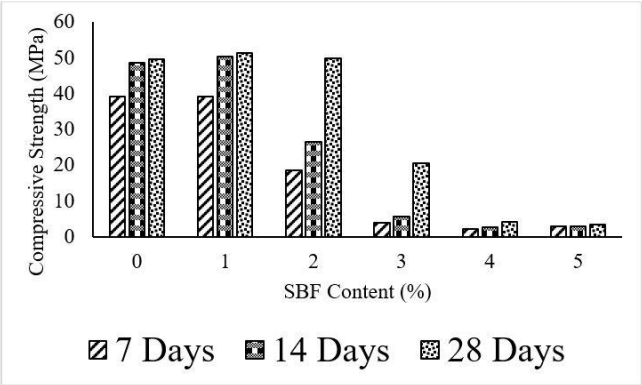

Fig 6. Compressive Strength of SBF-Cs

Bii. Flexural Strength (FS) and Splitting Tensile Strength (STS)

Bii(a) Flexural Strength (FS)

Flexural strength findings of all mixes with the splitting tensile strength are presented in Fig 7. During the process of concrete hydration, flexural strength is anticipated to increase progressively. Fig 7, illustrates the impact of adding sugarcane bagasse fiber on the flexural strength of the mixes. While the compressive strength of the modified concrete decreases as the fiber content increases, there is little difference in the pattern of the flexural strength results of the composite concrete mixes obtained. The flexural strength of the control concrete specimen is 5.55 MPa.

In comparison, mixtures with different fiber contents (1%, 2%, 3%, 4%, and 5%) have flexural strengths of 5.95 MPa, 5.84 MPa, 3.75 MPa, 1.47 MPa, and 0.86 MPa, respectively. Based on this outcome, increasing the flexural strength by utilizing sugarcane bagasse fiber at contents of 1% and 2% individually has a beneficial impact. However, when the loading is increased beyond that, there is a decrease in strength. The observed outcome can be attributed to the same factors extensively discussed concerning compressive strength: insufficient bonding between the aggregate and the sugarcane bagasse fiber, clusters of fibers, increased porosity, and the fracturing of fragile sugarcane bagasse fiber. The compact sugarcane bagasse fiber exhibits limited surface area, resulting in insufficient mechanical grip and physical interlocking with the aggregate.

Furthermore, sugarcane bagasse fiber has a limited chemical affinity for adhering to the cement matrix. Due to this factor, beams that include sugarcane bagasse fiber experience decreased flexural strength. According to Zakaria et al. [61], the study reported a reduction in the flexural strength of cementitious compositions containing various natural fibers similar to the report of this present study. In their study, Sridhar et al. [62] observed that the flexural strength of jute/bamboo reinforced concrete beams increased by up to 2% fiber content. However, when the fiber load was applied in an upward direction, it resulted in a decrease in strength. The incorporation of fibers in concrete aids in the development of flexural strength, provided that the fibers have a particular content and length. Furthermore, when the fiber is mixed with the concrete, it becomes clumped, making it difficult to distribute it evenly throughout the mixture. This uneven distribution of fiber becomes more pronounced when higher amounts of fiber are used, leading to a decrease in the flexural strength of the concrete [63].

Bii(b) Splitting Tensile Strength (STS)

Splitting tensile strength test results, which were carried out on both plain concrete and sugarcane bagasse fiber concretes at 28 days of concrete age, are illustrated in Fig 7, from which a similar trend to that of flexural strength is observed with a slight rise in splitting tensile strength from 1% to 2% fiber loading. However, it dropped after reaching the 2% reinforcement content compared to the control specimen. Incorporating sugarcane bagasse fiber into regular concrete resulted in a marginal enhancement in the tensile strength, particularly at lower fiber concentrations. The reference specimen's tensile strength value (STS) is measured as 3.13 MPa.

In comparison, the STSs of SBF-Cs with fiber contents of SBF-C-1%, SBF-C-2%, SBF-C-3%, SBF-C-4%, and SBF-C-5% were 3.47, 3.35, 0.71, 0.32, and 0.29 MPa, respectively. Adding 1% and 2% sugarcane bagasse fiber to the concrete increased its STS by 10% and 6.57%, respectively. Sugarcane bagasse fiber in low concentration helps bridge cracks and prevent their growth. However, further increasing the fiber content to 3%, 4%, and 5% reduced splitting tensile strength by 77.32%, 89.84%, and 90.67%, respectively. The increase in the strength of concrete is ascribed to the overall phenomenon that occurs when fiber reinforcement boosts the tensile capacity of the material. Conversely, the fall in strength is caused by establishing a weaker interfacial transition zone between the fibers and the matrix. The study conducted by Katman et al. [64] about using coir fiber-reinforced concrete supports the findings of this present study on sugarcane bagasse fiber.

Biii. Regression Analysis

The compressive strength of sugarcane bagasse fiber-concrete, fiber loading, flexural strength, and splitting tensile strength obtained after 28 days of curing were analyzed using regression modelling, with the result as expressed Tables II. The coefficient of determination (R^2) is a crucial indicator for evaluating the efficiency and efficacy of a system. The R^2 value, ranging from 0 to 1, quantifies the degree of precision between the model and the actual data. The relationship between fit and value is positively correlated, meaning that a higher fit level is associated with a lower value. Table II contains the regression analysis and analysis of variance of all the compressive strength models expressed below including R^2 as well as other additional assessments of the components inside the models. The regression model for compressive strength of the combined influence of variables flexural strength (FS), splitting tensile strength (STS) and fiber content (FC) has an R^2 value of 99.8%, multiple R 99.9%, adjusted R of 99.4%. These findings suggest that mathematical frameworks possess the capacity and capability to appropriately predict reactions. Table III to Table X expresses the different analysis of variance and coefficients for regression models.

CS = 0.697 – 0.915 Fiber Content + 4.506 FS + 7.380 STS
CS = 58.55 – 11.48 Fiber Content
CS = -9.33 + 10.04 FS
CS = 2.78 + 14.42 STS

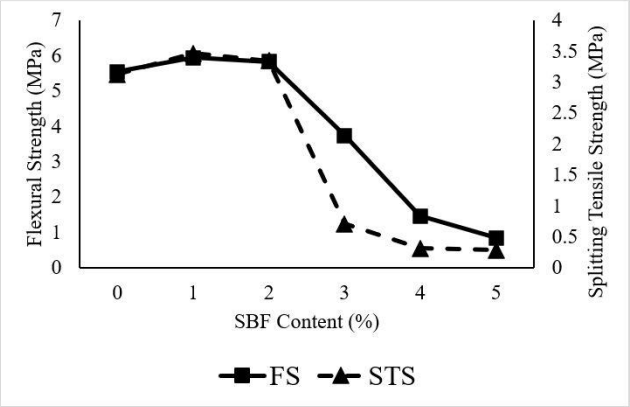

Fig 7. Flexural and Splitting Tensile Strengths of SBF-C

Table II: Regression Analysis

Regression Statistics				
	CS vs (FC, FS, STS)	CS vs FC	CS vs FS	CS vs STS
Multiple R	0.999	0.924	0.983	0.984
R Square	0.998	0.854	0.966	0.969
Adjusted R Square	0.994	0.818	0.957	0.961
Standard Error	1.85	9.925	4.803	4.597
Observations	6	6	6	6

Table III: ANOVA of model of Compressive Strength (FC, FS, STS)

	df	*SS*	*MS*	*F*	*Significance F*
Regression	3	2691.807	897.269	263.237	0.004
Residual	2	6.817	3.409		
Total	5	2698.624			

Table IV: Intercepts of models on Compressive Strengths against FC, FS, and STS

	Coefficients	*Standard Error*	*t Stat*	*P-value*
Intercept	0.697	6.206	0.112	0.921
Fiber Content	-0.915	1.119	-0.818	0.499
FS	4.506	1.263	3.569	0.070
STS	7.380	1.563	4.723	0.042

Table V: ANOVA of model of Compressive Strength vs FC

	df	*SS*	*MS*	*F*	*Significance F*
Regression	1	2304.61	2304.61	23.396	0.008
Residual	4	394.014	98.503		
Total	5	2698.624			

Table VI: Intercepts of models on Compressive Strengths against FC

	Coefficients	*Standard Error*	*t Stat*	*P-value*
Intercept	58.551	7.183	8.151	0.001
Fiber Content	-11.476	2.373	-4.837	0.008

Table VII: ANOVA of model of Compressive Strength vs FS

	df	*SS*	*MS*	*F*	*Significance F*
Regression	1	2606.333	2606.333	112.961	0.0004
Residual	4	92.2913	23.073		
Total	5	2698.624			

Table VIII: Intercepts of models on Compressive Strengths against flexural strength

	Coefficients	*Standard Error*	*t Stat*	*P-value*
Intercept	-9.327	4.176	-2.233	0.089
FS	10.0397	0.945	10.628	0.0004

Table IX: ANOVA of Model of Compressive Strength vs STS

	df	*SS*	*MS*	*F*	*Significance F*
Regression	1	2614.092	2614.092	123.697	0.0004
Residual	4	84.5321	21.133		
Total	5	2698.624			

Table X: Intercepts of models on Compressive Strengths against STS

	Coefficients	*Standard Error*	*t Stat*	*P-value*
Intercept	2.782	3.074	0.905	0.4166
STS	14.42	1.296	11.122	0.0004

C Acoustic Properties

Ci. Sound Absorption Coefficient (SAC)

The sound absorption coefficient is a vital metric in the field of acoustics. It quantifies the effectiveness of a material in absorbing sound energy when subjected to an acoustic wave. This dimensionless coefficient varies between 0 and 1,

with 0 representing complete reflection (no absorption) and 1 indicating complete absorption (all incoming sound energy is absorbed). The sound absorption coefficient is not constant and changes depending on the frequency because different materials and structures interact with sound waves at various frequencies within the spectrum. As illustrated in Fig 8, sugarcane bagasse fiber-reinforced concretes display the characteristic behavior of a bulk fibrous sound-absorbing material, where the sound-absorption coefficient increases with frequency up to a maximum value. Sugarcane bagasse fiber effectively improves the sound absorption coefficient (α) and enhances the sound insulation performance of the concrete specimens.

The concrete specimens comprising sugarcane bagasse fibers absorbed more sound than the plain concrete across the frequency range. Three frequencies can be observed as frequencies of high sound absorption coefficients, i.e., 1000 Hz, 4000 Hz, and 5600 Hz, as expressed in Fig 8. At 5600 Hz, the sound absorption coefficients of concretes produced with SBFs at fiber loads of 1, 2, 3, 4 and 5% were 0.18, 0.29, 0.31, 0.37 and 0.49, respectively, compared to plain concrete with a sound absorption coefficient of 0.13 which amounts to percentage increases in sound absorption of 28%, 55%, 58%, 65%, and 74% respectively as sugarcane bagasse fiber increases.

The result shows that plain concrete has a relatively weak sound absorption capability due to its dense structure and low porosity. However, when sugarcane bagasse fibers are incorporated, the absorption coefficient increases significantly with the increasing content of sugarcane bagasse fibers due to the increase in the porosity of the fiber-reinforced concrete which serves as a conduit to received sound energy turning it to heat energy as a result of friction between the pore walls and entrapped air within the pores. Also, the hollow structure or large porosity of SBFs, as previously shown in the SEM image of the fiber, explains the higher sound absorption in sugarcane bagasse fibers-reinforced concrete mixes than in standard concrete mixtures. This hollow structure traps and absorbs sound that enters the matrix, thereby increasing the sound absorption of concrete composites [65]-[66].

Consequently, SBFs in the concrete matrix increase its sound absorption capacity by providing cavities as sound trappers. The fibers themselves vibrate more readily and contribute to the rapid conversion of sound energy into heat energy [67].

Cii. Sound Absorption Average and Noise Reduction Coefficient.

Fig 9, illustrates the combined graph presentation of the sound absorption average, and the noise reduction coefficient of plain concrete and sugarcane bagasse fiber concrete obtained from the values of sound absorption coefficients attained at the different applied frequencies using (1) and (2), respectively. This study's plain concrete sound absorption average (SAA) is 0.061. This value is consistent with the range of sound absorption coefficients for typical concrete, as Khankhaje et al. [68] reported.

Incorporating sugarcane bagasse into the concrete mixture demonstrates a noticeable positive alteration to the SAA, concretes with a fiber substitution range of 1% to 5% fine aggregate replacement has SAA values range of 0.067 – 0.102, a percentage increase range of 10% - 67.2%. A constant increase in the SAA was observed with each incremental increase in fiber percentage. The chart indicates that the highest sound absorption average was achieved at 5% fiber/sand replacement.

SBF-concrete's noise reduction coefficient (NRC) increases gradually as the content of incorporated fibers replacing fine aggregate increases from 1% to 5%, as shown in Fig 9. The observed outcome demonstrates a substantial rise, increasing from 0.058 to 0.103. This increase equates to a significant 16 - 76% improvement in the percentage increase in sugarcane bagasse fiber-concrete noise reduction coefficient compared to plain concrete, as fiber content increases from 1% - 5%. The observed increase in NRC can be explained by the increased volume of fibers, which creates more paths for the dissipation of high sound energy through increased friction within the fiber-cement matrix. Composite concrete produced with sugarcane bagasse shows improved sound absorption capability compared to plain concrete.

Ciii. Comparative Study of Noise Reduction Coefficient

Table XI presents a comparative analysis of the noise reduction coefficient obtained from this study compared to

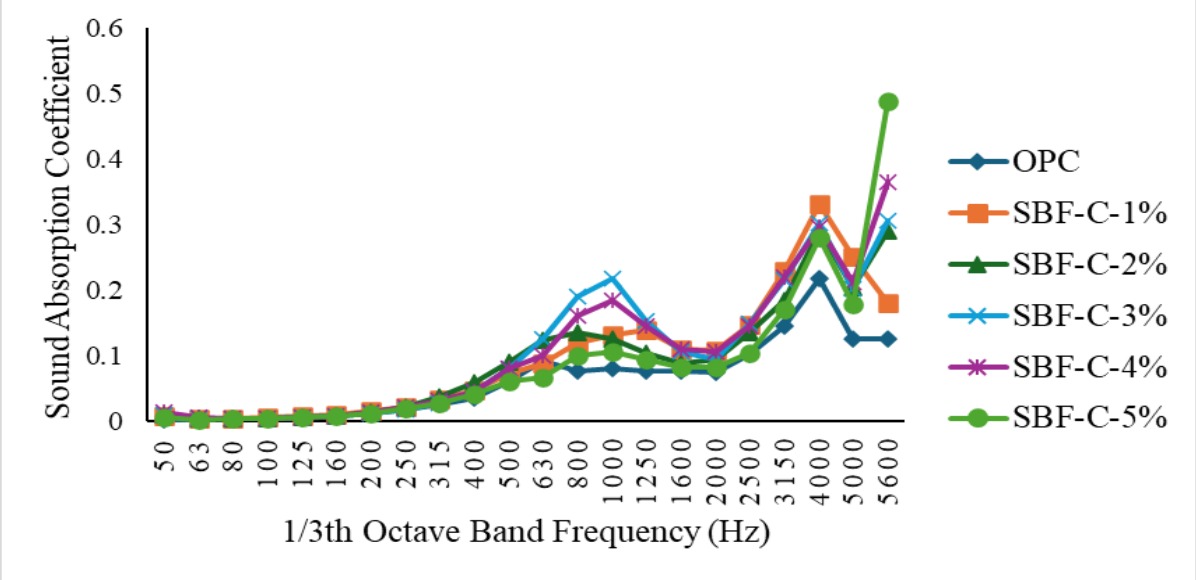

Fig 8. Sound Absorption Coefficient of SBF-Cs

comparable studies previously undertaken by other authors. This study's NRC is favorable compared to prior studies, as the values demonstrate a close-range proximity.

The utilization of sugarcane bagasse fiber, a natural fiber particle, in this study, can be compared favorably to the results obtained with concrete incorporated with miscanthus fibers conducted by Chen et al. [69].

The study demonstrates a reduction in the NRC at 20% fiber inclusion, which is lower than the NRC observed in this study at 5% fiber inclusion.

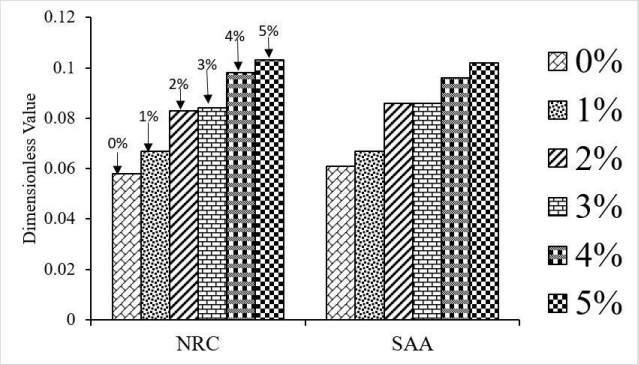

Fig 9. SAA and NRC of SBF-C

The superior performance of the NRC derived from sunflower (mc-sun) and corn waste (mc-corn) compared to the NRC obtained in this study is apparent. It is essential to highlight that the fiber particle sizes employed by Oancea et al. [70] were 40 mm, which exceeds the particle size range used in this study (0 – 1.18 mm). The presence of big particle sizes in their study resulted in larger voids, which in turn enhances the porosity of the specimens. This increased porosity facilitates air movement with less resistance, enabling a higher level of sound energy absorption within the specimens. Although the significant benefit of the substantial particle size is apparent, this investigation achieved an NRC value that closely aligns with the findings provided by Stolz et al. [71]. This finding demonstrates that including sugarcane bagasse fibers in concrete positively impacts sound energy absorption, decreasing the overall noise the listener perceives.

D. Porosity and Water Absorption of SBF-C Specimens

Fig 10 illustrates the result of the porosity test conducted on sugarcane bagasse fiber-reinforced concrete specimens. Porosity determination assists in evaluating the magnitude of pores within the specimens, a factor that significantly contributes to the attenuation of sound energy during their utilization. The porosity of the control specimen is observed to be 17.5%, while those of sugarcane bagasse fiber-concretes attained porosities of 16.2, 16.4, 18.1, 18.9, and 20.3%, representing porosity at fiber contents of 1, 2, 3, 4 and 5% respectively. The result shows an initial reduction followed by a steady and gradual increase in porosity levels compared to plain concrete, as quantified by percentage change. The measured percentage changes in porosity as the fiber loading increase of 1%, 2%, 3%, 4%, and 5% were -7.4%, -6.3%, +3.4%, +8%, and +16%, respectively, compared to plain concrete.

The observed increase in porosity can be attributed to the larger pore volume within the concrete sample. The increase in porosity can be attributed to the direct result of the augmented surface area resulting from the addition of the fiber to the concrete mixture. Furthermore, an augmentation in the fiber content leads to a higher quantity of notable interfacial transition zones at the boundary between the solidified cement paste and the fibers. More interconnected pores with different scales inside the composite concrete are created with the increased content of sugarcane bagasse fibers.

Table XI: Comparative Analysis of Related Studies

Authors	Type of fiber	Concrete Identifier	NRC
This study	**SBF**	**SBF-Concrete**	**0.06 – 0.103**
Oancea et al. 2018 [70]	Natural fibers	mc-corn 40 mm	0.193
		mc-sun 40mm	0.177
		mc-wool 40mm	0.178
Luna-Galiano et al. 2018 [72]	Geopolymer concrete	FA80SF20 – KOH 40°C	0.16 ± 0.01
		FA80SF20-KSil 40°C	0.14 ± 0.01
Xie et al., 2022 [73]		0.8MPa	0.20
		1.0 MPa	0.20
Kim et al., 2018 [74]		SII	0.15
		SVI	0.19
Chen et al., 2017 [69]	Miscanthus fibers	10%	0.15
	Miscanthus fibers	20%	0.11
Stolz et al., 2019[75]	Wood Ash Cement Foam	0-20%	0.08 – 0.14
Medina et al [76]	Lightweight aggregate concrete	20, 40, 60 and 80% crumb rubber as aggregate replacement	0.05, 0.04, 0.06 and 0.05.
Ling et al., as reported by Tie et al. [77]	Lightweight aggregate concrete	10, 20, 30% crumb rubber (<4.75 mm) as aggregate replacement	0.07, 0.09 and 0.12
Buratti et al. [78]	Plaster with lightweight aggregate	10 mm thick of insulation plaster with 80% aerogel	0.06
Zhang et al. [79]	Alkali-activated cellular concrete	5 and 10% foam dosage	0.10 and 0.12

Likewise, entrapped air, air holes, or pores are formed during compaction by fiber balling, creating more pores at interfaces. Therefore, it is evident that an increase in the fiber content results in a proportional increase in the overall porosity of the concrete specimens. According to Alemu et al. [80], porous materials have a better sound absorption capacity. SBF in concrete increases the composite concrete's porosity, resulting in better sound absorption performance.

Water absorption, often known as WA, is a fundamental characteristic of concrete that directly influences its durability and lifespan. The mix's composition, the length of curing, the amount of air present, and the addition of chemical and mineral admixtures are just a few factors that affect concrete's water absorption [81]. Fig 10 illustrates the water absorption of concrete with sugarcane bagasse fiber, from which it can be deduced that the inclusion of sugarcane bagasse fiber initially decreases the water absorption of the

concrete until a specific amount of fiber content is reached. However, beyond that threshold, the water absorption progressively rises as the fiber content increases. The decrease in water absorption may be observed consistently, with an increase in additional fibers resulting in higher water absorption than the plain concrete control specimen. The water absorption of sugarcane bagasse fiber-reinforced concrete decreases to 13.52%, 4.31%, and 2.92% at concentrations of 1%, 2%, and 3%, respectively. Increasing the fiber content to 4% and 5% led to a significant increase in water absorption by 35.72% and 48%, respectively, compared to plain concrete.

The first decline in water absorption compared to plain concrete indicates a decrease in accessible pores with a lower fiber load. Nevertheless, with an increase in fiber content, the microstructure of the concrete experiences the formation of more pores and air voids, resulting in heightened porosity and water absorption. In addition, the increased fiber content in the concrete results in enhanced uptake of free water by its fibrils due to its hydrophilic properties. As a result, water absorption is ultimately increased.

A study by Machaka et al. [82] found that adding phragmites australis fibers to composite concrete at a 0.5% to 1.5% loading rate caused a drop in water absorption (WA). This study found the same pattern. According to the study by Behera et al. [83], adding eucalyptus pulp and basalt fibrous waste to a hybrid-reinforced cement composite reduces the water absorption, but only by a maximum of 2%; however, further increases in fiber load led to a rise in water absorption.

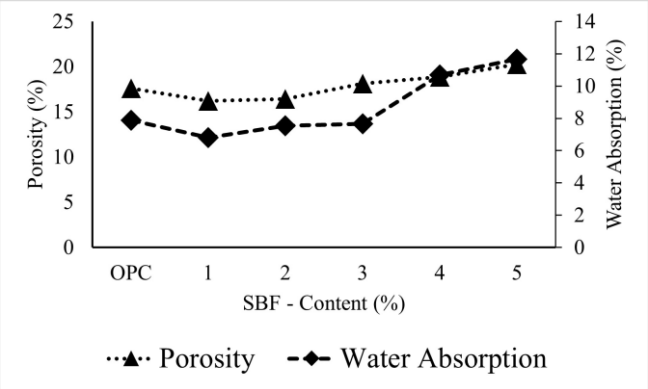

Fig 10. SBF-C Sound Absorption Test Specimens Porosity and Water Absorption.

E. Scanning Electron Microscopy

The SEM images are used to analyze the microstructure of the produced sugarcane bagasse fiber-reinforced concrete to evaluate the impact of partially replacing fine aggregate with SBF. Fig 11a displays the scanning electron microscope morphology of plain concrete. In contrast, Fig 11b-f illustrates the modified sugarcane bagasse fiber concrete morphology at different fiber replacement percentages: 1%, 2%, 3%, 4%, and 5%, respectively.

The incorporation of sugarcane bagasse fibers into concrete mixtures and the dispersion of these fibers within the structures created pores. The SEM images in Fig 11b-f depict a sequence of pore gaps in concrete formed using fiber/sand replacements. Void spaces are observed between fibers and cement binders at the interfacial transition zones. As a result, adding sugarcane bagasse fiber to the concrete matrix creates new interfaces between the fibers and matrix, leading to weak connections and void spaces between these constituents' components. These voids, spaces, and cavities allow for effective sound absorption because they act as pathways for the dissipation of sound energy [84].

Higher fiber inclusion percentages result in additional gaps and pore spaces within the concrete matrix and the fibers' microfibrils, increasing the capacity for sound absorption.

F. Electron Dispersive X-ray (EDX)

Energy-dispersive X-ray spectroscopy (EDX) examination was conducted to determine the types and semi-quantities of the constituent materials in concrete. The outcome of this test for plain concrete is presented in Fig 12a, whereas the results for SBF-C specimens are illustrated in Figs. 12b-f, with the specific percentage composition detailed in Table XII.

Fig 12 confirms the presence of calcium, magnesium, aluminium, silica, oxygen, carbon, silicon, and other components in the formed concrete structure. The incremental carbon percentage in the SBF-C corroborates the rise in fibre loading of the produced concretes.

G. Electron Dispersive X-ray (EDX)

Energy-dispersive X-ray spectroscopy (EDX) examination was conducted to determine the types and semi-quantities of the constituent materials in concrete. The outcome of this test for plain concrete is presented in Fig 12a, whereas the results for SBF-C specimens are illustrated in Figs. 12b-f, with the specific percentage composition detailed in Table XII.

Fig 12 confirms the presence of calcium, magnesium, aluminium, silica, oxygen, carbon, silicon, and other components in the formed concrete structure. The incremental carbon percentage in the SBF-C corroborates the rise in fibre loading of the produced concretes.

H. Thermogravimetric Analysis

The weight loss of plain concrete and SBF-C at different fibre loading rates was monitored and analysed using Thermo-Gravimetric Analysis (TGA) utilising the decomposition temperature. The thermal analysis was performed within the temperature range of 0 to 1000℃ comparable to what was reported by other study [85]. Thermogravimetric analysis was employed to assess the heat impact on the degradation of concrete. Figure 13a presents the thermal analysis of the control specimen, whereas Figure 13b depicts the thermal analysis results for SBF-C specimens.

The decomposition of concrete's constituents varies; calcium hydroxide (CH) in the cement paste decomposes at temperatures between 410 and 520℃, whereas the decomposition temperatures of other compounds, such as calcium silicate hydrate (C-S-H) and calcium silicate aluminate hydrate (C-S-A-H), are estimated to range from 100℃ to 390℃, as reported in the literature [86]. The TGA curve indicates that the thermal behaviour of SBF-C remains rather stable from 0℃, exhibiting a gradual minimum degradation until the first significant decomposition occurs at 435.83℃.

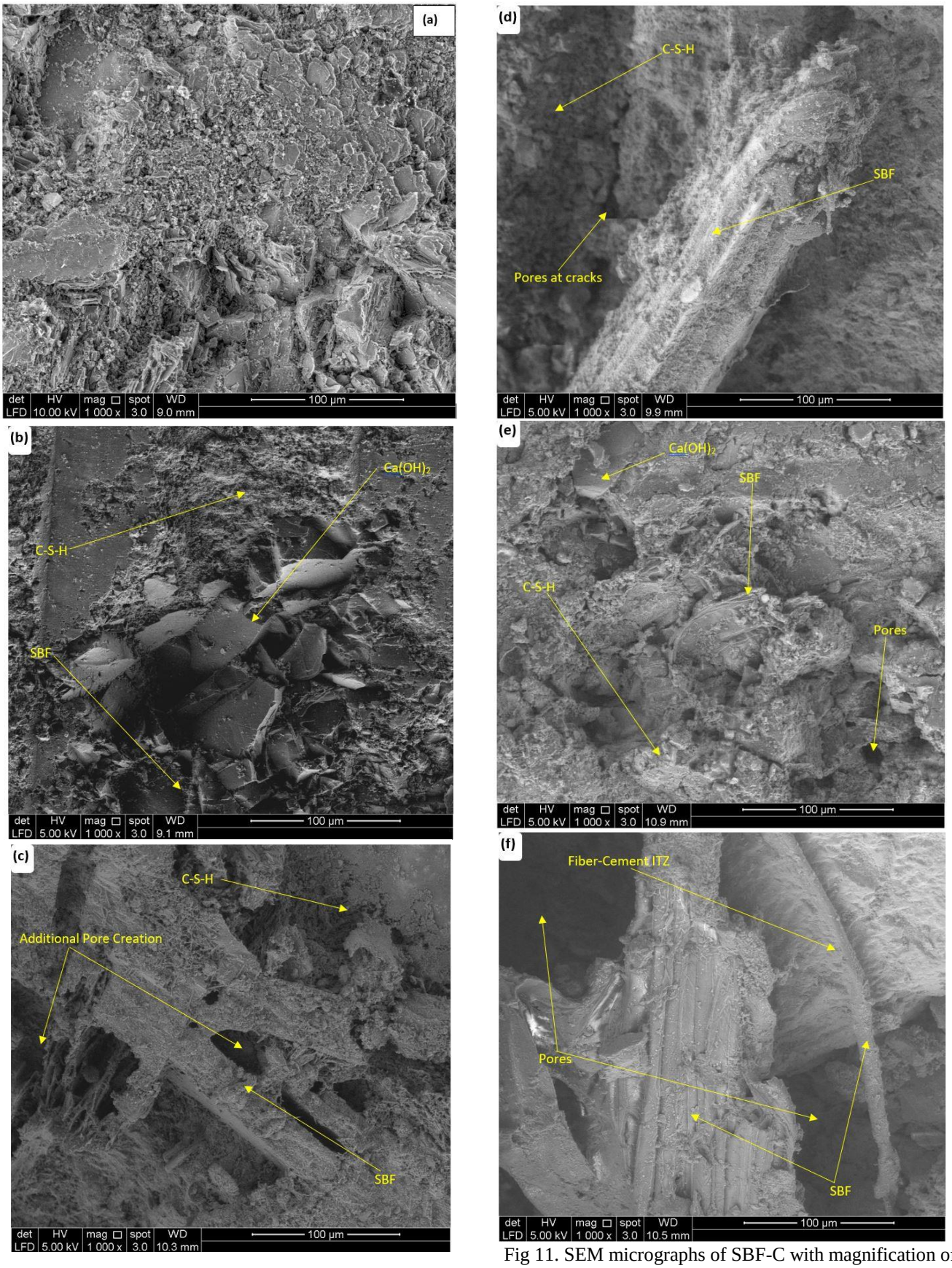

Fig 11. SEM micrographs of SBF-C with magnification of x1000: (a) plain concrete (b) SBF-C-1 (c) SBF-C-2 (d) SBF-C-3 (e) SBF-C-4 (f) SBF-C-5

At lower decomposition temperatures between 0 and 120℃, the evaporation of water within the structure of this concrete occurred for both plain and sugarcane bagasse fibre oncrete. The depletion of water at this temperature has been previously shown [87].

The decomposition of sugarcane bagasse fibre transpires between 200 to 400℃, resulting from the cleavage of glycosidic bonds in cellulose, the disintegration of lignin, and the degradation of hemicellulose [88]. The significant

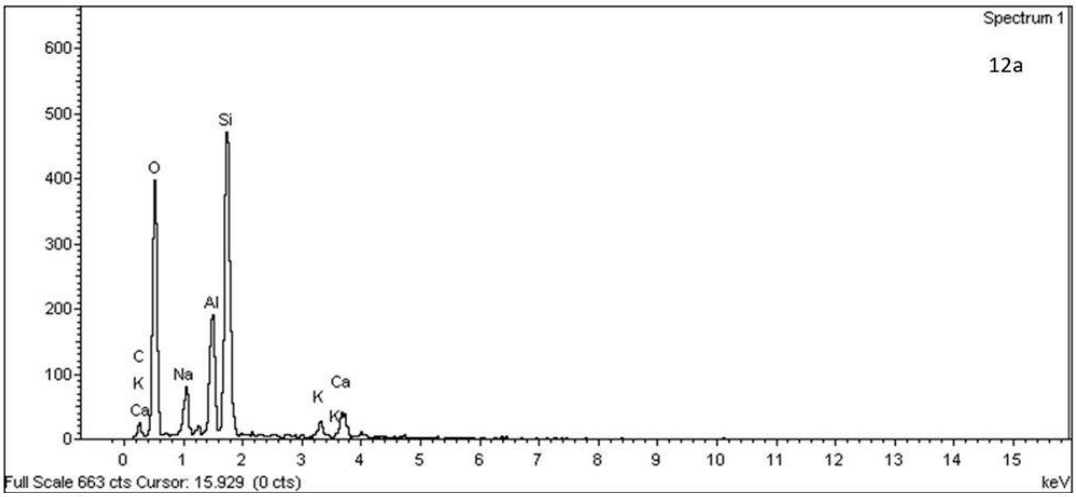
Spectrum 1
12a
O
Si
Al
C
K
Ca
Na
K
Ca
K
Full Scale 663 cts Cursor: 15.929 (0 cts)
keV

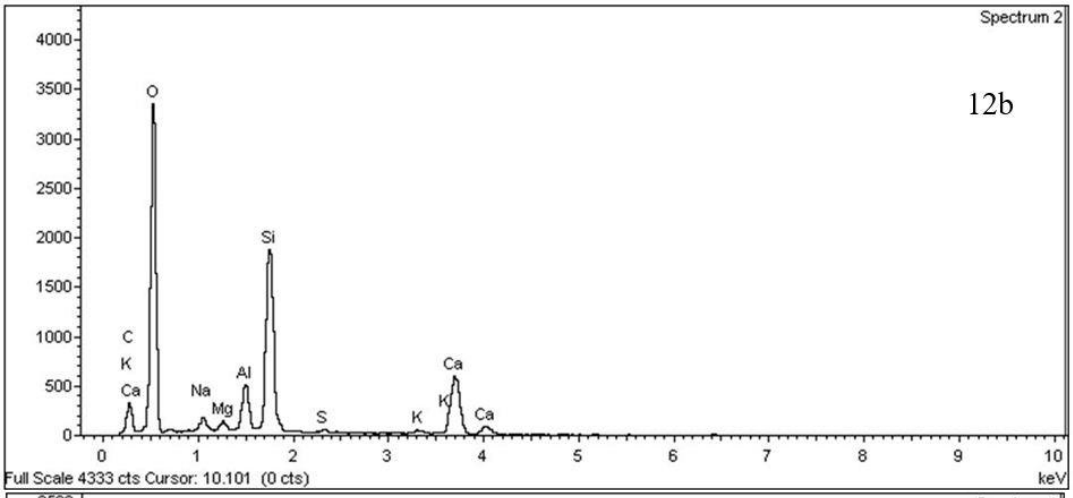
Spectrum 2
12b
O
Si
C
K
Ca
Al
Na
Mg
S
K
Ca
K
Ca
Full Scale 4333 cts Cursor: 10.101 (0 cts)
keV

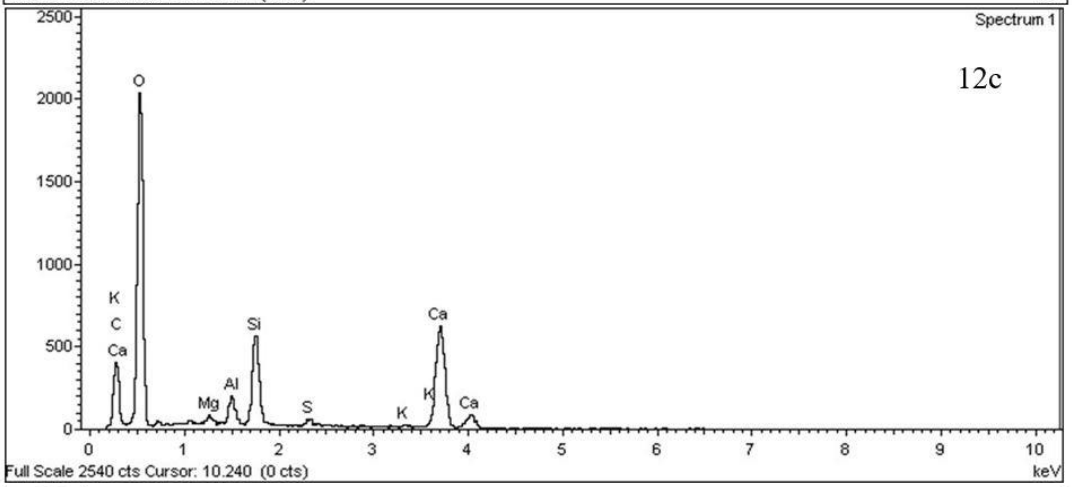
Spectrum 1
12c
O
K
C
Ca
Si
Al
Mg
S
K
Ca
K
Ca
Full Scale 2540 cts Cursor: 10.240 (0 cts)
keV

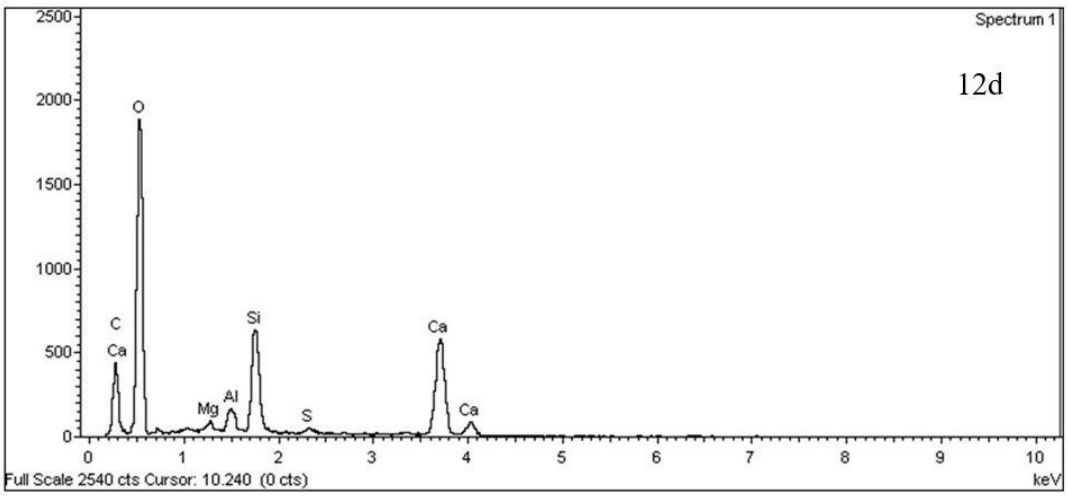
Spectrum 1
12d
O
C
Ca
Si
Al
Mg
S
Ca
Ca
Full Scale 2540 cts Cursor: 10.240 (0 cts)
keV

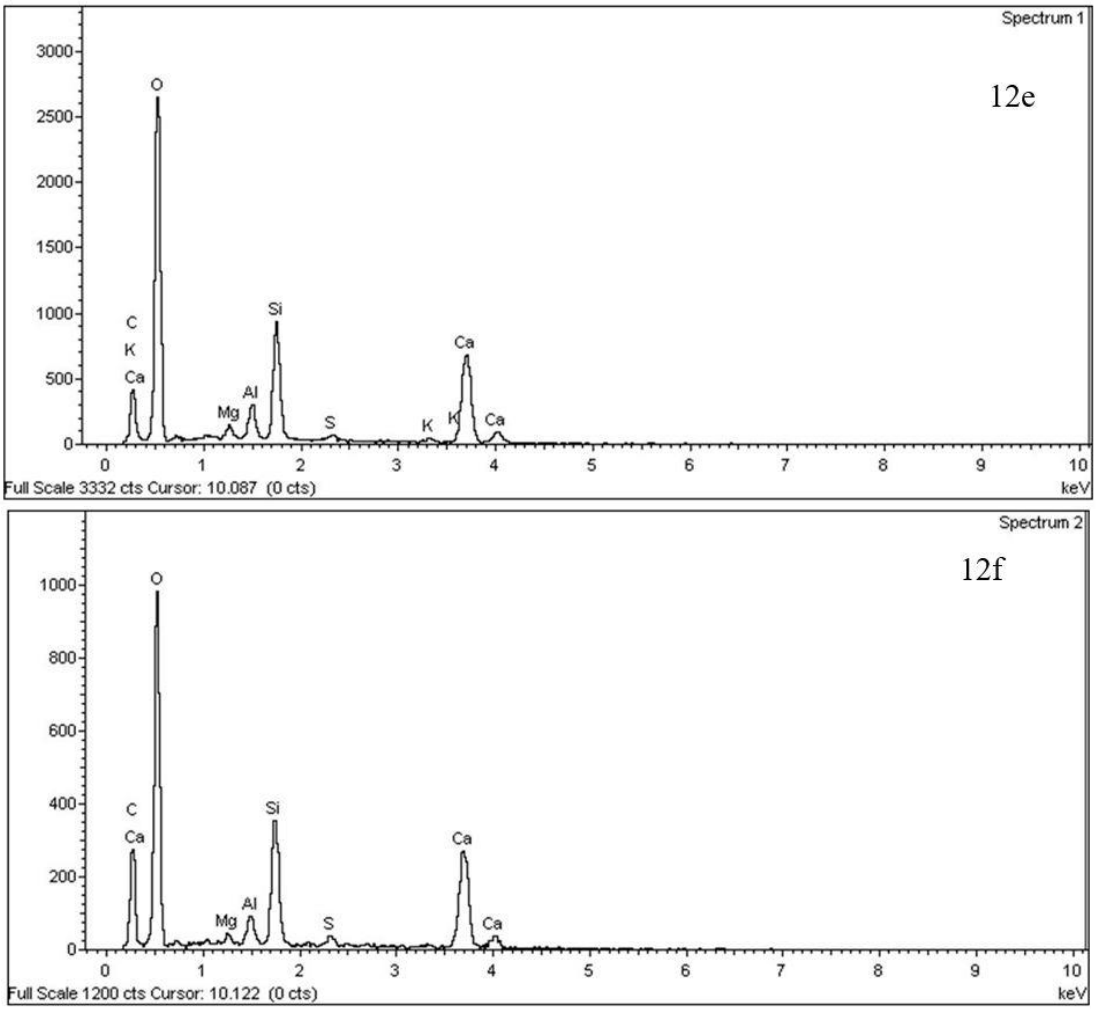

Fig 12: EDX Spectral of Concrete (a) Plain concrete; (b) SBF-C-1%, (c) SBF-C-2%, (d) SBF-C-3%, (e) SBF-C-4%, (f) SBF-C-5%

thermal degradation of other components in plain concrete and SBF-Cs occurred between temperatures of 430℃ and 718℃, attributed to the dissolution of calcium carbonate in the concrete matrix, consistent with the prior study by Kumar et al. [89].

Table XII: Elemental composition of sugarcane bagasse concrete

		Specimens					
Element	SBF	OPC	1	2	3	4	5
Ca		5.45	17.97	26.70	26.36	24.70	23.57
Na		5.01	1.01				
K		2.36	0.76	0.43		0.70	
C	51.20	0.00	7.04	10.39	10.21	10.98	13.77
Al	0.26	10.21	3.36	1.78	1.56	2.16	1.61
Mg	0.18		0.55	0.43	0.57	0.84	0.52
Si	0.23	29.68	16.63	7.19	8.77	9.31	9.01
O	48.14	47.29	52.27	52.41	51.98	50.8	50.54
S			0.41	0.69	0.55	0.51	0.96
Total	100	100	100	100	100	100	100

The residual materials following the decomposition process for ordinary concrete constitute 73%, but those for SBF-Cs vary between 74% and 81%. Compounds containing calcium were previously identified in the EDX data, which is corroborated by the TGA results. Overall, the weight loss of specimen after thermal analysis at 1000℃ for both plain concrete and SBF-C are 27% and 20 -25% respectively.

IV. CONCLUSION

The effect of partial replacement of fine aggregate by sugarcane bagasse fiber incorporation as concrete's constituents on the sound absorption coefficient and other properties was investigated. The results of this study can be summarized as follows:

1. The partial replacement of fine aggregate with SBF reduced the workability of the fresh concrete as the fiber content increased with a reduction percentage in the slump range of 3.4%—46% compared to the control, as fiber loading increased from 1%—5%.
2. Addition of 1-2% fiber content increases the compressive strength at 28 days by 3.28% and 0.66% respectively while fiber loading 3, 4 and 5% exerts a reduction in the compressive strength to 58.73, 91.54 and 92.95% respectively compared to plain concrete (49.67 MPa).
3. Both flexural strength and splitting tensile strength slightly increase at low fiber content, but an increase in fiber content beyond 2% resulted in a drastic reduction in strength.
4. The sound absorption coefficient (SAC) of produced SBF-Cs is more significant than that of plain concrete, which is clear evidence of the influence of fiber incorporation. The SAC percentage improvement ranges

from 28% to 55%, 58%, 65%, and 74%, representing positive percentage improvement at 1, 2, 3, 4, and 5% fiber loading in the SBF-C, respectively.

5. The inclusion of SBF in concrete resulted in the additional formation of pores within the concrete's microstructure as shown by SEM
6. SBF addition exerts slight reduction of porosity of concretes at low fiber content followed by a positive percentage increase in the range -7.4%, -6.3%, +3.4%, +8%, and +16%, representing fiber loads of 1, 2, 3, 4, and 5%, respectively, compred to plain concrete.
7. TGA shows consistency in the weight loss of specimens for both plain concrete and SBF-C valued at 27% and 20 -25% respectively.

Sugarcane bagasse fiber, a natural fiber, enhances the sound absorption performance of concrete composites fabricated with it as a component. Sugarcane bagasse fiber-concrete with a specific fiber content is suitable for use in the construction industry as both structural elements and noise barriers to mitigate environmental noise pollution.

REFERENCES

[1] Kolya, H., & Kang, C. W. (2021). Hygrothermal treated paulownia hardwood reveals enhanced sound absorption coefficient: An effective and facile approach. *Applied Acoustics*, *174*, 107758.

[2] Murphy, E., & King, E. A. (2022). *Environmental noise pollution: Noise mapping, public health, and policy*. Elsevier.

[3] Cuthbertson, D., Berardi, U., Briens, C., & Berruti, F. (2019). Biochar from residual biomass as a concrete filler for improved thermal and acoustic properties. *Biomass and bioenergy*, *120*, 77-83

[4] Faulkner, J. P., & Murphy, E. (2022). Estimating the harmful effects of environmental transport noise: An EU study. *Science of The Total Environment*, *811*, 152313.

[5] Redondo, J., Peiró-Torres, M. P., Llinares, C., Bravo, J. M., Pereira, A., & Amado-Mendes, P. (2021). Correlation between objective and subjective assessment of noise barriers. *Applied Acoustics*, *172*, 107640.

[6] Dissanayake, D. G. K., Weerasinghe, D. U., Thebuwanage, L. M., & Bandara, U. A. A. N. (2021). An environmentally friendly sound insulation material from post-industrial textile waste and natural rubber. *Journal of Building Engineering*, *33*, 101606.

[7] Kim, H., Hong, J., & Pyo, S. (2018). Acoustic characteristics of sound absorbable high performance concrete. *Applied Acoustics*, *138*, 171-178.

[8] Brown, A. L., & Van Kamp, I. (2017). WHO environmental noise guidelines for the European region: A systematic review of transport noise interventions and their impacts on health. *International journal of environmental research and public health*, *14*(8), 873.

[9] Wothge, J., Belke, C., Möhler, U., Guski, R., & Schreckenberg, D. (2017). The combined effects of aircraft and road traffic noise and aircraft and railway noise on noise annoyance—An analysis in the context of the joint research initiative NORAH. *International journal of environmental research and public health*, *14*(8), 871.

[10] Singh, D., Kumari, N., & Sharma, P. (2018). A review of adverse effects of road traffic noise on human health. *Fluctuation and Noise Letters*, *17*(01), 1830001.

[11] Morillas, J. M. B., Gozalo, G. R., González, D. M., Moraga, P. A., &

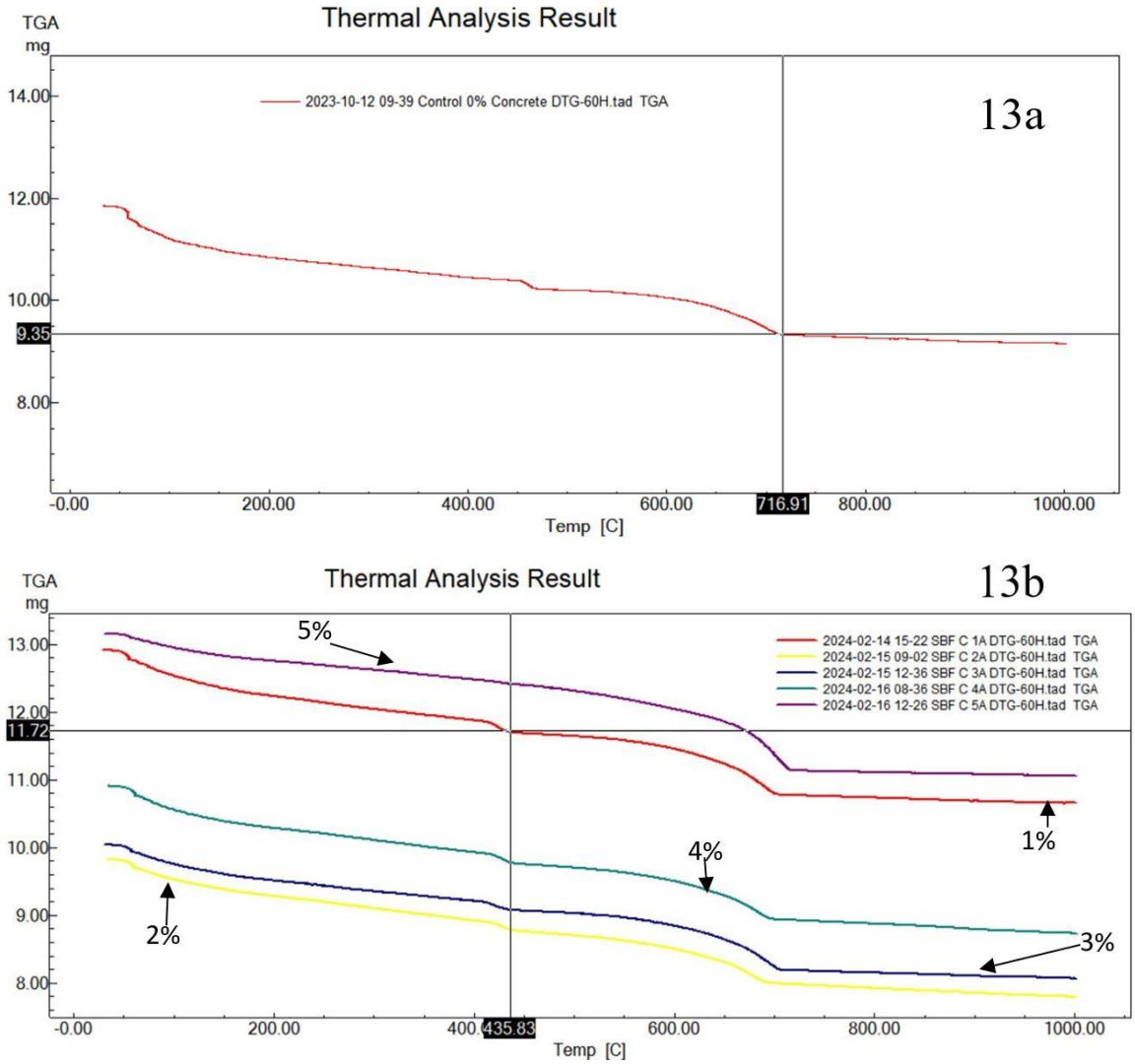

Fig 13: TGA of specimens (a) Plain concrete (b) SBF-C-(1% -5%)

Vílchez-Gómez, R. (2018). Noise pollution and urban planning. *Current Pollution Reports*, *4*(3), 208-219.

[12] Evandt, J., Oftedal, B., Krog, N. H., Skurtveit, S., Nafstad, P., Schwarze, P. E., ... & Aasvang, G. M. (2017). Road traffic noise and registry based use of sleep medication. *Environmental health*, *16*, 1-12.

[13] Skrzypek, M., Kowalska, M., Czech, E. M., Niewiadomska, E., & Zejda, J. E. (2017). Impact of road traffic noise on sleep disturbances and attention disorders amongst school children living in Upper Silesian Industrial Zone, Poland. *International journal of occupational medicine and environmental health*, *30*(3), 511-520.

[14] Dzhambov, A., Tilov, B., Markevych, I., & Dimitrova, D. (2017). Residential road traffic noise and general mental health in youth: The role of noise annoyance, neighborhood restorative quality, physical activity, and social cohesion as potential mediators. *Environment international*, *109*, 1-9.

[15] Cheng, L., Wang, S. H., Huang, Y., & Liao, X. M. (2016). The hippocampus may be more susceptible to environmental noise than the auditory cortex. *Hearing research*, *333*, 93-97.

[16] Christensen, J. S., Raaschou-Nielsen, O., Tjønneland, A., Nordsborg, R. B., Jensen, S. S., Sørensen, T. I., & Sørensen, M. (2015). Long-term exposure to residential traffic noise and changes in body weight and waist circumference: a cohort study. *Environmental research*, *143*, 154-161.

[17] Odugbose, B. D., Akinyemi, O. O., Sule, S. O., & Babalola, A. A. (2019). Sound effects of occupational noise exposure on personnel in burr mill processing centres. *FULafia Journal of Science and Technology*, *5*(2), 120-125.

[18] Herni Halim, Ramdzani Abdullah, and Mohd. Jailani Mohd Nor, Hamidi Abdul Aziz, Noorhazlinda Abd Rahman (2017). Comparison Between Measured Traffic Noise In Klang Valley, Malaysia And Existing Prediction Models. *Engineering Heritage Journal / Galeri Warisan Kejuruteraan* , 1(2):10–14

[19] Alyousef, R. (2022). Enhanced acoustic properties of concrete composites comprising modified waste sheep wool fibers. *Journal of Building Engineering*, *56*, 104815.

[20] Lim, N. H. A. S., Mohammadhosseini, H., Tahir, M. M., Samadi, M., & Sam, A. R. M. (2018). Microstructure and strength properties of mortar containing waste ceramic nanoparticles. *Arabian Journal for Science and Engineering*, *43*, 5305-5313.

[21] Kaish, A. B. M. A., Odimegwu, T. C., Zakaria, I., & Abood, M. M. (2021). Effects of different industrial waste materials as partial replacement of fine aggregate on strength and microstructure properties of concrete. *Journal of Building Engineering*, *35*, 102092.

[22] Amran, M., Fediuk, R., Murali, G., Vatin, N., & Al-Fakih, A. (2021). Sound-absorbing acoustic concretes: A review. *Sustainability*, *13*(19), 10712.

[23] Shtrepi, L., Astolfi, A., Badino, E., Volpatti, G., & Zampini, D. (2021). More than just concrete: acoustically efficient porous concrete with different aggregate shape and gradation. *Applied Sciences*, *11*(11), 4835.

[24] Rodrigues, P. C., de Sales Braga, N. T., Junior, E. S. A., Cordeiro, L. D. N. P., & de Melo, G. D. S. V. (2022). Effect of pore characteristics on the sound absorption of pervious concretes. *Case Studies in Construction Materials*, *17*, e01302.

[25] Abu-Jdayil, B., Mourad, A. H., Hittini, W., Hassan, M., & Hameedi, S. (2019). Traditional, state-of-the-art and renewable thermal building insulation materials: An overview. *Construction and Building Materials*, *214*, 709-735.

[26] Alam, M. A., & Al Riyami, K. (2018). Shear strengthening of reinforced concrete beam using natural fiber reinforced polymer laminates. *Construction and Building Materials*, *162*, 683-696.

[27] Asim, M., Uddin, G. M., Jamshaid, H., Raza, A., Hussain, U., Satti, A. N., ... & Arafat, S. M. (2020). Comparative experimental investigation of natural fibers reinforced light weight concrete as thermally efficient building materials. *Journal of Building Engineering*, *31*, 101411.

[28] de Azevedo, A. R., Marvila, M. T., Tayeh, B. A., Cecchin, D., Pereira, A. C., & Monteiro, S. N. (2021). Technological performance of açaí natural fiber reinforced cement-based mortars. *Journal of Building Engineering*, *33*, 101675.

[29] Yang, T., Hu, L., Xiong, X., Petrů, M., Noman, M. T., Mishra, R., & Militký, J. (2020). Sound absorption properties of natural fibers: A review. *Sustainability*, *12*(20), 8477.

[30] Wang, S., Li, H., Zou, S., Liu, L., Bai, C., Zhang, G., & Fang, L. (2022). Experimental study on durability and acoustic absorption performance of biomass geopolymer-based insulation materials. *Construction and Building Materials*, *361*, 129575.

[31] Chen, Y., Yu, Q. L., & Brouwers, H. J. H. (2017). Acoustic performance and microstructural analysis of bio-based lightweight concrete containing miscanthus. *Construction and Building Materials*, *157*, 839-851

[32] Chen, Y. X., Wu, F., Yu, Q., & Brouwers, H. J. H. (2020). Bio-based ultra-lightweight concrete applying miscanthus fibers: Acoustic absorption and thermal insulation. *Cement and Concrete Composites*, *114*, 103829

[33] Pachla, E. C., Silva, D. B., Stein, K. J., Marangon, E., & Chong, W. (2021). Sustainable application of rice husk and rice straw in cellular concrete composites. *Construction and Building Materials*, *283*, 122770.

[34] Oancea, I., Bujoreanu, C., Budescu, M., Benchea, M., & Grădinaru, C. M. (2018). Considerations on sound absorption coefficient of sustainable concrete with different waste replacements. *Journal of Cleaner Production*, *203*, 301-312.

[35] ACI (American Concrete Institute) Committee 318. 2019. Building Code Requirements for Structural Concrete (ACI 318-19) and Commentary (ACI 318R-19). Farmington Hills, MI: ACI

[36] Karolina, R., Muharrisa, R., & Handana, M. A. P. (2020). The effect of rice straw fiber addition as sound silencer and its effect to concrete mechanical properties. In *IOP Conference Series: Materials Science and Engineering* (Vol. 725, No. 1, p. 012035). IOP Publishing

[37] ASTM. (2020). ASTM C143/C143M: Standard test method for slump of hydraulic-cement concrete. West Conshohocken, PA, USA: American Society of Testing and Materials

[38] ASTM C642-21 *Standard Test Method for Density, Absorption, and Voids in Hardened Concrete*. Retrieved February 7 2024, from https://www.astm.org/c0642-21.html

[39] BSI. (2009). BS EN 12390-3: Testing hardened concrete. Part 3: Compressive strength of test specimens.

[40] ASTM, C. (2002). 78-02. Standard test method for flexural strength of concrete (using simple beam with third–point loading). *Annual Book of ASTM Standards, American Society for Testing and Materials*.

[41] ASTM C 496/C 496M-04, *Standard Test Method for Splitting Tensile Strength of Cylindrical Concrete Specimens*, American Standard Test Method, West Conshohocken, Penn, USA, 2004

[42] ASTM C1202-22. (n.d.). *Standard Test Method for Electrical Indication of Concrete's Ability to Resist Chloride Ion Penetration*. Retrieved 7 February 2024, from https://www.astm.org/c1202-22e01.html

[43] ASTM E1050. Standard Test Method for Impedance and Absorption of Acoustical Materials Using a Tube, Two Microphones and a Digital Frequency Analysis System; American Society for Testing and Materials: West Conshohocken, PA, USA, 2012.

[44] Maderuelo-Sanz, R., Nadal-Gisbert, A. V., Crespo-Amorós, J. E., Morillas, J. M. B., Parres-García, F., & Sanchis, E. J. (2016). Influence of the microstructure in the acoustical performance of consolidated lightweight granular materials. *Acoustics Australia*, *44*, 149-157.

[45] Carbajo San Martín, J., Esquerdo-Lloret, T. V., Ramis-Soriano, J., Nadal-Gisbert, A. V., & Denia, F. D. (2015). Acoustic properties of porous concrete made from arlite and vermiculite lightweight aggregates.

[46] Samaei, S. E., Berardi, U., Taban, E., Soltani, P., & Mousavi, S. M. (2021). Natural fibro-granular composite as a novel sustainable sound-absorbing material. *Applied Acoustics*, *181*, 108157.

[47] Nastac, S., Nechita, P., Debeleac, C., Simionescu, C., & Seciureanu, M. (2021). The acoustic performance of expanded perlite composites reinforced with rapeseed waste and natural polymers. *Sustainability*, *14*(1), 103.

[48] Raj, M., Fatima, S., & Tandon, N. (2020). A study of areca nut leaf sheath fibers as a green sound-absorbing material. *Applied Acoustics*, *169*, 107490.

[49] ASTM Standard C830-00 e1: Standard Test Methods for Apparent Porosity, Liquid absorption, Apparent specific Gravity, and Bulk Density of Refractory Shapes by Vacuum Pressure, ASTM Annual Book of Standards, 2006, Vol. 15.01.

[50] Arenas, C., Ríos, J. D., Cifuentes, H., Vilches, L. F., & Leiva, C. (2022). Sound absorbing porous concretes composed of different solid wastes. *European Journal of Environmental and Civil Engineering*, *26*(9), 3805-3817.

[51] Shojaei, T. R., Soltani, S., & Derakhshani, M. (2022). Synthesis, properties, and biomedical applications of inorganic bionanomaterials. In *Fundamentals of bionanomaterials* (pp. 139-174). Elsevier.

[52] Kaddah, F., Roziere, E., Ranaivomanana, H., & Amiri, O. (2023). Complementary use of thermogravimetric analysis and oven to assess the composition and bound CO2 content of recycled concrete aggregates. *Developments in the Built Environment*, *15*, 100184.

[53] Ali, M., Liu, A., Sou, H., & Chouw, N. (2012). Mechanical and dynamic properties of coconut fibre reinforced concrete. *Construction and Building Materials*, *30*, 814-825.
[54] Ahmed, M. F. (2024). Exploring the characteristics and effects of date palm waste on some properties of concrete: a review. *Kufa Journal of Engineering*, *15*(1), Article 1. https://doi.org/10.30572/2018/kje/150104
[55] Subedi, S., Arce, G. A., Noorvand, H., Hassan, M. M., Barbato, M., & Mohammad, L. N. (2021). Properties of Engineered Cementitious Composites with Raw Sugarcane Bagasse Ash Used as Sand Replacement. *Journal of Materials in Civil Engineering*, *33*(9), 04021231. https://doi.org/10.1061/(ASCE)MT.1943-5533.0003892
[56] Mohamed, O. A., & Hawat, W. A. (2016). Influence of Fly Ash and Basalt Fibers on Strength and Chloride Penetration Resistance of Self-Consolidating Concrete. *Materials Science Forum*, *866*, 3–8. https://doi.org/10.4028/www.scientific.net/MSF.866.3
[57] Priya, C., & Sudalaimani, K. (2023). Performance assessment of surface modified natural fibre using NaOH in composite concrete. *Materials Research Express*, *10*(12), 125101. https://doi.org/10.1088/2053-1591/ad1076
[58] Zeyad, A. M., Megat Johari, M. A., Tayeh, B. A., & Yusuf, M. O. (2016). Efficiency of treated and untreated palm oil fuel ash as a supplementary binder on engineering and fluid transport properties of high-strength concrete. *Construction and Building Materials*, *125*, 1066–1079. https://doi.org/10.1016/j.conbuildmat.2016.08.065
[59] Odugbose Babashola Dapo, Herni Binti Halim, and Izwan Johari, "Experimental Investigation of the Effect of Elaeis guineensis Mesocarp Fiber on Physical, Mechanical and other Selected Properties of Natural-Fiber Reinforced-Concrete," Engineering Letters, vol. 32, no. 2, pp379-391, 2024
[60] Shon, C. S., Mukashev, T., Lee, D., Zhang, D., & Kim, J. R. (2019). Can common reed fiber become an effective construction material? Physical, mechanical, and thermal properties of mortar mixture containing common reed fiber. *Sustainability*, *11*(3), 903.
[61] Zakaria, M., Ahmed, M., Hoque, M., & Shaid, A. (2018). A comparative study of the mechanical properties of jute fiber and yarn reinforced concrete composites. *Journal of Natural Fibers*.
[62] Sridhar, J., Gobinath, R., & Kırgız, M. S. (2022). Comparative study for efficacy of chemically treated jute fiber and bamboo fiber on the properties of reinforced concrete beams. *Journal of Natural Fibers*, *19*(15), 12224-12234.
[63] Sultana, N., Hossain, S. Z., Alam, M. S., Hashish, M. M. A., & Islam, M. S. (2020). An experimental investigation and modeling approach of response surface methodology coupled with crow search algorithm for optimizing the properties of jute fiber reinforced concrete. *Construction and Building Materials*, *243*, 118216.
[64] Katman, H. Y. B., Khai, W. J., Bheel, N., Kırgız, M. S., Kumar, A., & Benjeddou, O. (2022). Fabrication and characterization of cement-based hybrid concrete containing coir fiber for advancing concrete construction. *Buildings*, *12*(9), 1450.
[65] Ghermezgoli, Z. M., Moezzi, M., Yekrang, J., Rafat, S. A., Soltani, P., & Barez, F. (2021). Sound absorption and thermal insulation characteristics of fabrics made of pure and crossbred sheep waste wool. *Journal of Building Engineering*, *35*, 102060.
[66] Kobiela-Mendrek, K., Bączek, M., Broda, J., Rom, M., Espelien, I., & Klepp, I. (2022). Acoustic performance of sound absorbing materials produced from wool of local mountain sheep. *Materials*, *15*(9), 3139.
[67] Zhang, Y., Li, H., Abdelhady, A., & Yang, J. (2020). Effect of different factors on sound absorption property of porous concrete. *Transportation Research Part D: Transport and Environment*, *87*, 102532.
[68] Khankhaje, E., Salim, M. R., Mirza, J., Hussin, M. W., Khan, R., & Rafieizonooz, M. (2017). Properties of quiet pervious concrete containing oil palm kernel shell and cockleshell. *Applied Acoustics*, *122*, 113-120.
[69] Chen, Y., Yu, Q. L., & Brouwers, H. J. H. (2017). Acoustic performance and microstructural analysis of bio-based lightweight concrete containing miscanthus. *Construction and Building Materials*, *157*, 839-851.
[70] Oancea, I., Bujoreanu, C., Budescu, M., Benchea, M., & Grădinaru, C. M. (2018). Considerations on sound absorption coefficient of sustainable concrete with different waste replacements. *Journal of Cleaner Production*, *203*, 301-312.
[71] Stolz, J., Boluk, Y., & Bindiganavile, V. (2018). Mechanical, thermal and acoustic properties of cellular alkali activated fly ash concrete. *Cement and Concrete Composites*, *94*, 24-32.
[72] Luna-Galiano, Y., Leiva, C., Arenas, C., & Fernández-Pereira, C. (2018). Fly ash based geopolymeric foams using silica fume as pore generation agent. Physical, mechanical and acoustic properties. *Journal of non-crystalline solids*, *500*, 196-204
[73] Xie, H., Li, Y., Kahya, E., Wang, B., Ge, X., & Li, G. (2022). Physical Properties and Environmental Impact of Sound Barrier Materials Based on Fly Ash Cenosphere. *Buildings*, *12*(3), 322.
[74] Kim, H., Hong, J., & Pyo, S. (2018). Acoustic characteristics of sound absorbable high performance concrete. *Applied Acoustics*, *138*, 171-178.
[75] Stolz, J., Boluk, Y., & Bindiganavile, V. (2019). Wood ash as a supplementary cementing material in foams for thermal and acoustic insulation. *Construction and Building Materials*, *215*, 104-113.
[76] Medina, N. F., Flores-Medina, D., & Hernández-Olivares, F. (2016). Influence of fibers partially coated with rubber from tire recycling as aggregate on the acoustical properties of rubberized concrete. *Construction and building Materials*, *129*, 25-36.
[77] Tie, T. S., Mo, K. H., Putra, A., Loo, S. C., Alengaram, U. J., & Ling, T. C. (2020). Sound absorption performance of modified concrete: A review. *Journal of Building Engineering*, *30*, 101219.
[78] Buratti, C., Moretti, E., Belloni, E., & Agosti, F. (2014). Development of innovative aerogel based plasters: preliminary thermal and acoustic performance evaluation. *Sustainability*, *6*(9), 5839-5852.
[79] Zhang, Z., Provis, J. L., Reid, A., & Wang, H. (2015). Mechanical, thermal insulation, thermal resistance and acoustic absorption properties of geopolymer foam concrete. *Cement and Concrete Composites*, *62*, 97-105.
[80] Alemu, A. S., Yoon, J., Tafesse, M., Seo, Y. S., Kim, H. K., & Pyo, S. (2021). Practical considerations of porosity, strength, and acoustic absorption of structural pervious concrete. *Case Studies in Construction Materials*, *15*, e00764.
[81] Nematollahzade, M., Tajadini, A., Afshoon, I., & Aslani, F. (2020). Influence of different curing conditions and water to cement ratio on properties of self-compacting concretes. *Construction and Building Materials*, *237*, 117570.
[82] Machaka, M., Khatib, J., Baydoun, S., Elkordi, A., & Assaad, J. J. (2022). The Effect of Adding Phragmites australis Fibers on the Properties of Concrete [J]. Buildings 2022, 12, 278.
[83] Behera, P., Noman, M. T., & Petrů, M. (2020). Enhanced mechanical properties of eucalyptus-basalt-based hybrid-reinforced cement composites. *Polymers*, *12*(12), 2837.
[84] Debnath, B., & Sarkar, P. P. (2020). Pervious concrete as an alternative pavement strategy: A state-of-the-art review. *International Journal of Pavement Engineering*, *21*(12), 1516–1531. https://doi.org/10.1080/10298436.2018.1554217
[85] Xia, Y., Zhu, C., Ouyang, S. *et al*. Thermogravimetric characteristics and evaluation of products during pyrolysis of *Camellia oleifera* seed residues. *Biomass Conv. Bioref.* (2024). https://doi.org/10.1007/s13399-024-05342-6
[86] Zapata, J. F., Colorado, H. A., & Gomez, M. A. (2020). Effect of high temperature and additions of silica on the microstructure and properties of calcium aluminate cement pastes. *Journal of Sustainable Cement-Based Materials*, *9*(6), 323-349.
[87] Garcia-Lodeiro, I.; Irisawa, K.; Jin, F.; Meguro, Y.; Kinoshita, H. Reduction of water content in calcium aluminate cement with/out phosphate modification for alternative cementation technique. Cem. Concr. Res. **2018**, 109, 243–253.
[88] Xue, P., Liu, M., Yang, H., Zhang, H., Chen, Y., Hu, Q., ... & Chen, H. (2023). Mechanism study on pyrolysis interaction between cellulose, hemicellulose, and lignin based on photoionization time-of-flight mass spectrometer (PI-TOF-MS) analysis. *Fuel*, *338*, 127276.
[89] Kumar, V.; Singh, V.K.; Srivastava, A.; Agrawal, G.N. Low Temperature Synthesis of High Alumina Cements by Gel-Trapped Co-Precipitation Process and Their Implementation as Castables. J. Am. Ceram. Soc. **2012**, 95, 3769–3775.